

The Ultimate Fate of Supercooled Liquids

Jacob D. Stevenson^{1,2} and Peter G. Wolynes^{1,3}

¹*Department of Physics and Department of Chemistry and Biochemistry,
Center for Theoretical Biological Physics, University of California at San Diego, La Jolla, California 92093*

²*Institut für Physik, Johannes Gutenberg-Universität, 55099 Mainz, Germany*

³*e-mail: pwolynes@ucsd.edu*

(Dated: October 25, 2021)

In recent years it has become widely accepted that a dynamical length scale ξ_α plays an important role in supercooled liquids near the glass transition. We examine the implications of the interplay between the growing ξ_α and the size of the crystal nucleus, ξ_M , which shrinks on cooling. We argue that at low temperatures where $\xi_\alpha > \xi_M$ a new crystallization mechanism emerges enabling rapid development of a large scale web of sparsely connected crystallinity. Though we predict this web percolates the system at too low a temperature to be easily seen in the laboratory, there are noticeable residual effects near the glass transition that can account for several previously observed unexplained phenomena of deeply supercooled liquids including Fischer clusters, and anomalous crystal growth near T_g .

Thermodynamics tells us that the ultimate fate of a liquid held below its melting point is to crystallize. This notion is buttressed by the observation that terrestrial rocks are generally polycrystalline and the rare amorphous minerals found naturally are geologically young[1]. Nevertheless, amorphous solids are ubiquitous and while some atactic polymers or heteropolymers may not be able to crystallize at all because they have no plausible competing periodic crystal structure, most everyday glass substances are only kinetically prevented from crystallizing on human time scales. Understanding the competition between crystallization and glass formation is thus of great practical significance. Turnbull’s early ideas about this competition, based on augmenting nucleation theory with a dynamical correction from the viscous slowing of glassy liquids[2], have held up remarkably well, allowing the discovery and exploitation of metallic glasses[3, 4], among other things. Reasoning analogous to Turnbull’s inspired the energy landscape theory of protein folding, leading to the idea that proteins have evolved to avoid the kinetic traps expected for heteropolymers, allowing rapid formation of native structure[5]: the “minimal frustration principle.” Turnbull’s nucleation argument also implies a crisp time scale separation between crystallization and the quiescent equilibrium dynamics of a supercooled liquid. This time scale separation makes it possible to discuss an equilibrium supercooled liquid as defined by the Gibbs measure applied to that part of many body configuration space lacking supercritical crystallization nuclei. This restricted equilibrium description would be useful down to a temperature where thermodynamically barrierless or spinodal crystallization can occur.

Many features of the dynamics of metastable, “equilibrated” supercooled liquids, and of nonequilibrium glasses, have been understood using the random first order transition (RFOT) theory of the glass transition[6]. Generally, it has been possible, within the RFOT framework, to ignore the possibility of a periodic crystalline state. In this paper we explore how RFOT theory is modified when we account for the existence of a periodic crystalline state. These arguments suggest there is indeed a wide range of accessible thermodynamic con-

ditions where Turnbull’s analysis of nucleation should hold. These arguments predict, however, that even above the temperature where there is a strict spinodal, a new mechanism of crystallization should emerge that will compromise the usually assumed time scale separation between crystallization and structural (so called α) relaxation. When a substance has a periodic ground state, an approach to an ideal glass transition amongst the strictly amorphous structures is then predicted to ultimately be intercepted by crystallization in a kinetic sense.

The arguments in this paper hinge on the dynamical mosaic structure envisioned in RFOT theory. RFOT theory predicts the existence of a length scale for dynamical correlations that grows as the liquid is cooled. Long after this length scale was predicted, numerous experiments using NMR and imaging directly revealed such a length scale for dynamical heterogeneity[7–9]. The RFOT predicted length agrees with both those direct measurements and more indirect inferences of dynamical length scales[10, 11]. Since the dynamical correlation length grows on cooling, the scales of the dynamical mosaic at some point become comparable to the size of the classical crystallization nucleus which, in contrast, shrinks as the liquid becomes more deeply supercooled. Just below freezing, when the dynamical and nucleation length scales are well separated, the Turnbull nucleation picture is adequate. But upon deeper supercooling, when the scales cross, a new kind of local percolative “nanocrystallization” is predicted to occur, driven by the dynamical heterogeneity of the viscous liquid. At first, the nuclei will be sparse and grow slowly at a rate still controlled by α relaxation. A bit further cooling, however, allows another threshold to be crossed where the theory predicts more extensive crystal nucleation and considerably more rapid crystal growth, which while still slow in human terms, will be completely decoupled in time scale from α relaxation. In this regime a true α relaxation time for an equilibrium supercooled liquid would not be operationally defined.

These new regimes of crystallization explain several anomalous observations about supercooled liquids which suggest that supercooled liquids have bigger density variations

than would be expected on thermodynamic grounds. One such anomaly is the excess low angle x-ray scattering observed by Fischer’s group indicating fluctuations whose magnitude is inconsistent with the macroscopic compressibility[12]. Our picture ascribes this excess scattering to slow growing nanocrystallites. The nanocrystallites also explain the long environmental exchange times observed in some single molecule fluorescence experiments[13], that have so far not been observed using nonlinear NMR[9]. If sufficient time elapses, the nanocrystallites can grow to form a connected but fragile web[13], explaining anomalous solid-like elastic behavior at low shear, (which disappears on more vigorous flow) even above the nominal glass transition temperature. In this new regime, heterogeneous nucleation from the presence of foreign or seeded nuclei is also enhanced, explaining the quantitative inconsistencies between the various experiments that find such anomalous long-lived structures.

The present picture also predicts that crystal growth starting from heterogeneously nucleated crystals will abruptly change speed and mechanism upon sufficiently deep supercooling. Several experiments do show anomalously rapid crystal growth beginning near, but above, the laboratory glass transition[14–16].

The organization of the paper is as follows: we first reprise the “energy landscape library construction”[17], now accounting for the gap in the spectrum of states that arises from the existence of a particularly stable periodic structure. This argument defines the length scales for motions relevant to α relaxation, the classical crystallization nucleus size and a third critical size for forming nanocrystallites. The comparisons of these lengths allow us to delineate the crystallization regimes. Similar arguments for heterogeneous nucleation on foreign nuclei makes predictions for crystal growth which we compare to experiment. Finally, we discuss more general issues of phase separation and polyamorphism in glassy liquids as well as how these new mechanisms impinge on the design of glassy materials and on protein folding theory.

ENERGY LANDSCAPE LIBRARIES AND CRYSTALLIZATION

A liquid has a large diversity of structures, as manifested by an extensive configurational entropy. In figure 1, we show schematically the spectrum of local free energy minima of a large sample. Macroscopic crystalline states have an extensive gap separating them, in energy, from the liquid manifold. Since the thermally sampled states change with temperature, this gap is taken to be $\Delta\epsilon(T)N$ where N is the number of molecular units in the sample. At the melting point the magnitude of $\Delta\epsilon$ is accessible from calorimetry $\Delta\epsilon(T_m) = T_m S_c(T_m)$. For simplicity, we will generally speak of an energy landscape library, although more properly we should use the term (Gibbs) free energy landscape since local vibrational entropies should be included — indeed, for hard spheres, vibrational entropy provides the entirety of an

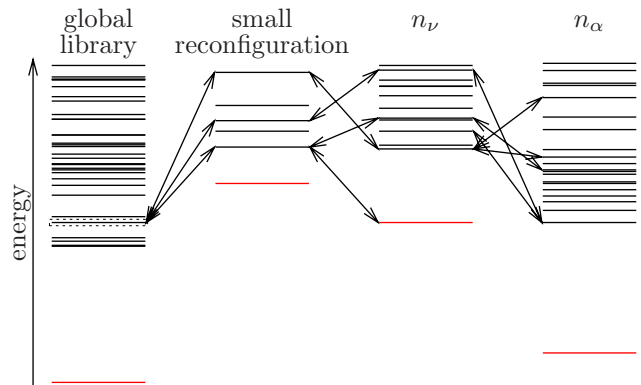


FIG. 1. A schematic diagram of the microcanonical energy landscape. The leftmost panel shows the global configuration of states with the crystal having the lowest energy. The second panel shows the distribution of energy levels after a small number of particles have reconfigured (starting from the boxed initial state). The energies are higher due to the surface mismatch penalty. The third panel shows the distribution of energies after n_ν particles have moved. Here the energy of the crystal nucleus is comparable to the initial state, but is destabilized by the entropy of the large number of amorphous configurations. The rightmost panel shows the distribution of energies after reconfiguring n_α particles. The arrows suggest possible pathways of reconfiguration.

individual minimum’s free energy.

Structural transitions occur through local rearrangements. Thus we must consider the changes of (free) energy and diversity that occur when only a finite number of particles, n , are moved. Instead of a single global energy landscape, there are thus numerous local energy landscape libraries as illustrated also in Fig 1. In general, when a small number of molecules move, the energy becomes higher than the initial minimum’s energy since the alternate geometry has steric conflicts with the original surroundings, now frozen, which can only be partially ameliorated by small harmonic deformations. Owing to the extensive configurational entropy, the size of the local library grows exponentially with the number of displaced particles n , and at some point, with increasing n , a structure of comparable energy to the original one will be found. If the energy gap is substantial, the first near resonant level to be encountered will be crystalline. We will call such a structure a “nanocrystallite.” It will contain n_ν particles. Although such a nanocrystallite can initially form locally, if the configurational entropy is high the newly formed nanocrystallite will quickly disappear, because although transitions to any of the other specific amorphous states is energetically uphill, such transitions are extraordinarily numerous — roughly there are $\exp\{n_\nu s_c/k_B\}$ of them, giving their net formation rate a large value.

Owing to its entropic disadvantage, a nanocrystallite, after forming, will revert to one of the set of amorphous members of the local library. It will then usually fall back downhill to the original amorphous structure since n is less than n_α . Of course, a distinct amorphous structure could become near resonant, and indeed this typically happens when n_α particles

are displaced, defining the size of a cooperatively rearranging region (of radius ξ_α). Eventually, as bulk thermodynamics dictates, the entropic disadvantage of a small nanocrystallite will be overcome by the growth with size of the energy gap, so a big enough nanocrystallite will not disappear, but grows, essentially irreversibly. This point of no return defines the classical critical nucleus for crystallization, n_M^\ddagger .

There are three different free energy curves to consider when thinking about local rearrangements of a supercooled liquid with a periodic crystalline ground state. These can be thought of as reflecting separate averages over the amorphous states and the periodic crystal states treated as reactants and products in a chemical reaction. (At this stage we will ignore the fluctuations in driving force that will modify these free energy profiles owing to the diversity of surrounding environments. Let us take, for concreteness, the mismatch energy of amorphous/amorphous pairings to scale like $\sigma_\alpha n^{y_\alpha}$ and the mismatch energy for the amorphous/crystal pairings to scale as $\sigma_x n^{y_x}$. Such pure power laws are oversimplifications. For compact reconfiguring clusters in three dimensions, the exponents in these expressions would be 2/3. RFOT theory suggests there are significant ‘‘wetting’’ corrections to these (mean field) results; these corrections may be large enough (near an ideal glass transition) to give an effective exponent of 1/2 rather than 2/3. While the most appropriate exponent is debated[11, 18–21], the distinction between various choices makes little difference to the present story, as we shall see. Likewise the crystallization mismatch energy exponent y_x would classically be expected to be 2/3, but could appear smaller if the crystallite’s surface is above its roughening transition.

The free energy for a reconfiguration event to any other amorphous state satisfies $F_\alpha = -Ts_c(T)n + \sigma_\alpha n^{y_\alpha}$. The reader is referred to the paper by Lubchenko and Wolynes[17] to see how the microcanonical rate of conversion to any *one* specific amorphous state is transformed to the rate for transiting to the ensemble of amorphous states (hence the driving force is $-Ts_c(T)$). The profile for transiting directly to a nanocrystallite (since a single definite starting state is involved) has the energy gap driving force, hence $F_\nu = -\Delta\epsilon(T)n + \sigma_x n^{y_x}$. Yet, if the numerous alternate amorphous structures can also be accessed by the disappearance of transient nanocrystallites and α relaxation processes, the bulk driving force will be that from an equilibrated ensemble of amorphous structures, i.e. per particle it is $-(\Delta\epsilon(T) - Ts_c(T))$, giving the total macroscopic nucleation free energy profile $F_M = -(\Delta\epsilon(T) - Ts_c(T))n + \sigma_x n^{y_x}$.

Each of the three curves defines characteristic sizes: n_M^\ddagger , the size of the macroscopic crystal transition state nucleus, n_α the size of a cooperatively rearranging amorphous region and n_ν the size of a nanocrystallite. Their values are found from the free energy profiles described above:

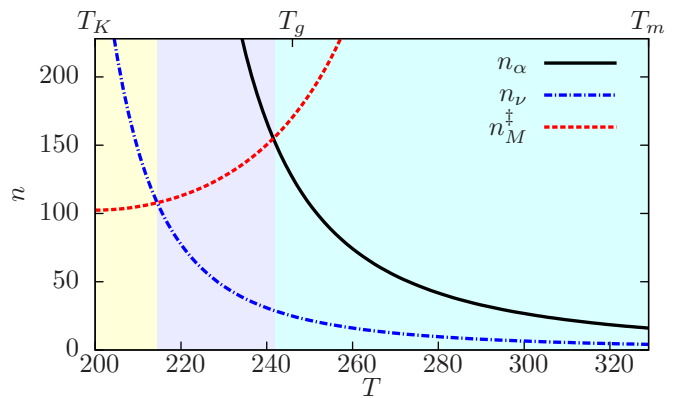


FIG. 2. The temperature dependence of n_α , the size of a typical amorphous reconfiguration; n_M^\ddagger , the transition state size of classical crystal nucleation; and n_ν , the number of particles involved in nanocrystallization. Within the shaded region on the right classical nucleation theory is valid. In the shaded region on the left direct nanocrystallization can take place. Crystallization in the center region takes place through fluctuational, percolative nanocrystallization.

$$\begin{aligned} n_\alpha &= \left(\frac{\sigma_\alpha}{Ts_c(T)} \right)^{\frac{1}{1-y_\alpha}} \\ n_\nu &= \left(\frac{\sigma_x}{\Delta\epsilon(T)} \right)^{\frac{1}{1-y_x}} \\ n_M^\ddagger &= \left(\frac{\sigma_x y_x}{\Delta\epsilon(T) - Ts_c(T)} \right)^{\frac{1}{1-y_x}}. \end{aligned} \quad (1)$$

As sketched in figure 2, n_α increases with decreasing T , and in contrast n_M^\ddagger decreases with decreasing T . The nanocrystallite size changes the least with temperature. Figures 2 and 4 are drawn using material parameters of the fragile liquid o-terphenyl, the details of which, as well as analogous curves for a strong glass former, can be found in the supplementary material.

Macroscopic nucleation only occurs at temperatures below the melting point T_m . Just below T_m the relationships between the three free energy profiles are as pictured in figure 3a. In this regime $n_M^\ddagger > n_\alpha > n_\nu$. Nanocrystallites constantly form and disappear either reverting to the initial amorphous state or becoming new amorphous structures in which n_α particles have moved. The macroscopic nucleation barrier at n_M^\ddagger is crossed by making many moves of size n_α . Thus the prefactor of the rate will be related to ω_α . In this high temperature regime the rates associated with each of the processes discussed are

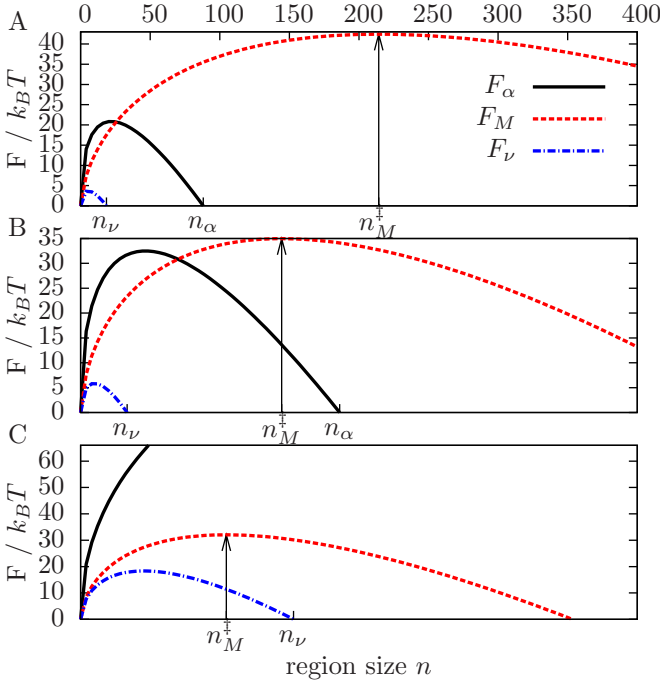


FIG. 3. Free energy profiles of α relaxation (F_α), bulk crystallization (F_M) and nanocrystallization (F_ν) at the three temperature regimes shaded in figure 2.

$$\begin{aligned}
 \omega_\alpha &= \omega_0 \exp \left\{ -\frac{\sigma_\alpha}{k_B T} \left(\frac{y_\alpha \sigma_\alpha}{T s_c(T)} \right)^{\frac{y_\alpha}{1-y_\alpha}} (1-y_\alpha) \right\} \\
 \omega_\nu &= \omega_0 \exp \left\{ -\frac{\sigma_x}{k_B T} \left(\frac{y_x \sigma_x}{\Delta \epsilon(T)} \right)^{\frac{y_x}{1-y_x}} (1-y_x) \right\} \\
 \omega_M &= \omega_\alpha \exp \left\{ -\frac{\sigma_x}{k_B T} \left(\frac{y_x \sigma_x}{\Delta \epsilon(T) - T s_c(T)} \right)^{\frac{y_x}{1-y_x}} (1-y_x) \right\}
 \end{aligned} \quad (2)$$

The prefactor for both ω_ν and ω_α is ω_0 , the rate of microscopic vibrations. The temperature dependence of the rates is shown in figure 4A. It should be noted that for the bulk crystallization rate the prefactor ought to be the average inverse α relaxation time, however for simplicity, we use the inverse typical relaxation time, underestimating the bulk crystallization rate, especially for lower temperatures.

The mechanism of nucleation changes when the supercooling is sufficient for n_α to exceed n_M^\ddagger , as shown in figure 3b and figure 3c, i.e. at T_{cross}^X , defined by

$$n_\alpha(T_{\text{cross}}^X) \equiv n_M^\ddagger(T_{\text{cross}}^X). \quad (3)$$

It can be seen from figure 2 that this crossover occurs near the laboratory T_g . This concurrence is fairly robust to the details of the liquid, but is a coincidence, since the one hour time scale used for the laboratory glass transition is anthropocentrically defined.

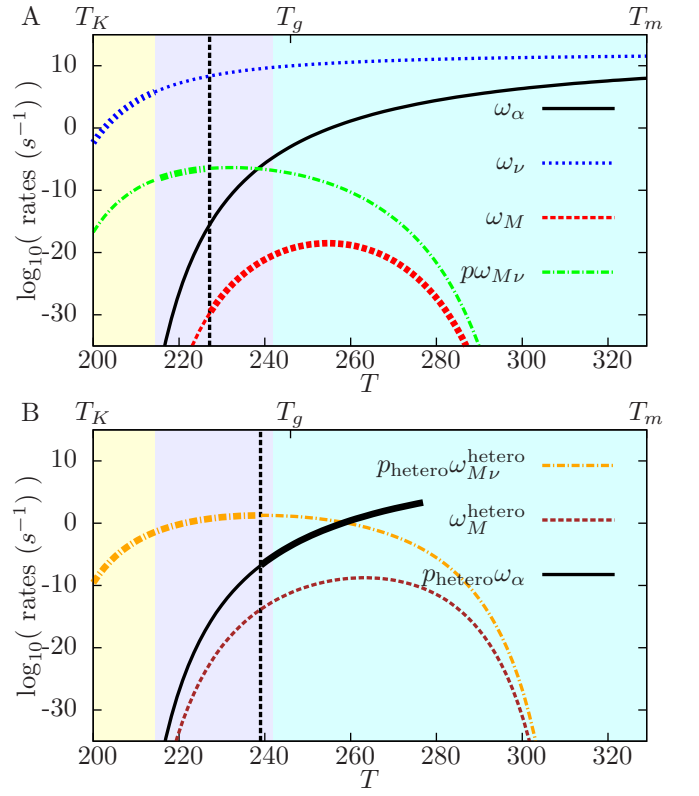


FIG. 4. Panel A shows the temperature dependence of nucleation rates for α relaxation (ω_α), bulk crystallization (ω_M), nanocrystallization (ω_ν), and percolative fluctuational nanocrystallization ($p\omega_{M\nu}$). The temperature regimes are shaded as per figure 2. The homogeneous percolation transition is marked with a vertical line. Rates are indicated as the inverse time to see a nucleation event within a microscopic volume. Since a single crystal nucleus would spread rapidly through the system the rate at which a sample of volume V would crystallize is $\sim \omega_M V$, a rate much faster than that appearing in the figure. Panel B shows rates for heterogeneous crystal surface nucleation. At high temperatures the surface nucleation rate is proportional to ω_α . At the heterogeneous percolation temperature (marked by a vertical line) the crystal growth rate switches to be $p_{\text{hetero}}\omega_{M\nu}^{\text{hetero}}$. For both panels the relevant rates for crystal nucleation and growth are emphasized with a thick line.

There are two somewhat different mechanisms of crystallization below the temperature T_{cross}^X where the traditional nucleation theory analysis breaks down. Which mechanism applies depends on the relative size of n_ν and n_M^\ddagger . Only at very low configurational entropies can we satisfy the strongest condition $n_\nu > n_M^\ddagger$. In this case, shown in figure 3c the nanocrystallite has no tendency to disappear at all. Once a nanocrystallite forms, it continues to grow without having a chance to access other amorphous structures. The critical temperature for in this extremely supercooled regime $n_\nu(T_{\text{crit}}) \equiv n_M^\ddagger(T_{\text{crit}})$ leads, through equation 1, to the relation

$$T_{\text{crit}} s_c(T_{\text{crit}}) = (1-y_x) \Delta \epsilon(T_{\text{crit}}). \quad (4)$$

It can be seen in figure 2 that this direct form of nanocrystal-

lization occurs significantly below T_g , at deep enough supercooling that it probably has not been observed in the laboratory, although it may occur in geology.

When crystals form from direct nanocrystallization rather than through the rearrangements of α relaxation, the prefactor for the nucleation rate will be ω_ν , rather than the much slower ω_α

$$\omega_{M\nu} = \omega_\nu \exp \left\{ -\frac{F_M^\ddagger(T)}{k_B T} \right\} \quad (5)$$

Were it possible to reach this regime of undercooling while remaining equilibrated in the amorphous ensemble, there would clearly be no dependence of crystallization rate on ω_α . The sample would completely crystallize at the rate $\omega_{M\nu}$ before any α relaxation time could be measured.

THE DYNAMICAL MOSAIC AND PERCOLATING NANOCRYSTALLITES

There is an intermediate regime not covered by the above cases. What happens when $n_\alpha > n_M^\ddagger$ but $n_M^\ddagger > n_\nu$ as shown in figure 3b? No single process dominates, so the answer depends on an interplay between length and time scales for the fluctuations. Typically a nanocrystallite, once formed, disappears, but no alternate amorphous structure can be stabilized at that location. Nevertheless since n_M^\ddagger is smaller than n_α , the nucleation threshold could still be crossed while remaining within the original local amorphous structure. According to RFOT theory, each region of size n_α can be thought of as having a variable but temporarily fixed energy [18, 22] (until its environment reconfigures). The magnitude of the energy variance of a region of size n follows from mesoscale statistical thermodynamics and is related to the configurational heat capacity, $T^2 k_B \Delta C_p / n$.

In some mosaic cells, the driving force will be sufficient for the nanocrystallite to cross the macroscopic crystal formation threshold. In those cells then, nanocrystallites will initially form. The density of these stable nanocrystallites will depend on $s_c(T_{\text{crit}})$, the critical entropy density for direct nanocrystallization that we have already discussed. We expect a fraction of mosaic cells

$$p = \frac{1}{2} \operatorname{erfc} \left\{ \frac{s_c(T) - s_c(T_{\text{crit}})}{\sqrt{2k_B \Delta C_p / n_\nu}} \right\} \quad (6)$$

will irreversibly nucleate in this manner. The temperature dependence of p is displayed in the supplementary material. If this nanocrystallization probability is big enough to allow percolation, a gossamer percolative network will form rapidly at the rate $p\omega_{M\nu}$. This has the effect of raising the lower critical temperature which signals the onset of rapid crystallization independent of the slow α relaxations. Even above this percolation transition temperature, if α relaxation is slow compared

with the nanocrystallite nucleation rate $p\omega_{M\nu}$, large, ramified networks of crystalline structure will appear, but remain finite in size. The details of crystal morphology in this regime involve a complicated interplay of length and time scales and deserve a more extensive treatment than is provided here. At high temperatures the formation of these crystalline networks will be broken up by amorphous reconfigurations, destroying any nascent long range order.

HETEROGENEOUS CRYSTAL NUCLEATION AND GROWTH ON PREEXISTING CRYSTALS

Any of the sparse, stable nanocrystallites, once formed, will be able to grow directly, in the manner of a chain reaction, if it has a further neighbor that is itself also sufficiently stable. Each step in a possible nucleation chain is actually a heterogeneous nucleation process. The presence of a nanocrystallite increases the rate at which its neighbors nucleate. Foreign particles or seed nuclei likewise make possible smaller critical nucleation sizes, and thus the percolative crystallization mechanism can begin at lower degrees of supercooling when seeds are present. If the seeds introduced are nanoscale, smaller than n_α in size, they can be thought of as adding a constant stability increment to the crystallization free energy profiles, increasing locally the driving force for nucleation, and allowing the nanocrystallite chain reaction route at a higher temperature than for strictly homogeneous nucleation.

The situation for still larger seed particles, those bigger than n_α , is somewhat more subtle. For nucleated crystal growth on a flat interface only a hemisphere of newly crystallized material need be laid down at a time [15, 23]. The disturbed volume is approximately half the volume for spherical growth $n_\nu^{\text{hetero}} \approx n_\nu / 2$. The propagation probability

$$p_{\text{hetero}} = \frac{1}{2} \operatorname{erfc} \left\{ \frac{s_c(T) - s_c(T_{\text{crit}})}{\sqrt{2k_B \Delta C_V / n_\nu^{\text{hetero}}}} \right\}, \quad (7)$$

is greater than p , since growth after the first nucleus is present is essentially a surface process. The degree of stabilization for growth on a curved surface will be somewhat smaller. A more general analysis would take $n_\nu / 2 \leq n_\nu^{\text{hetero}} \leq n_\nu$, but we restrict our discussion here to the limiting case. The rate for this heterogeneous percolative growth should be of order $p_{\text{hetero}}\omega_{M\nu}^{\text{hetero}}$ where

$$\omega_{M\nu}^{\text{hetero}} \approx \omega_\nu \exp \left\{ \frac{-F_M^\ddagger(T)}{2k_B T} \right\} \quad (8)$$

which is much faster than ω_α at low temperatures. The chain reaction mechanism ultimately turns off as s_c increases. After falling below the percolation criterion upon warming, crystal growth will proceed a finite distance before it is obliged to wait for the environment to reconfigure. Thus at high temperatures the growth is limited by the α relaxation rate and will

be proportional to $p_{\text{hetero}}\omega_{\alpha}$, as in figure 4. Since $p_{\text{hetero}}(T)$ crosses the percolation threshold at a higher temperature than $p(T)$, seed nuclei are sparse at this crossover temperature, leading to a noticeable period of aging during which ω_{α} can be measured, but eventually, as always the sample will crystallize. An analogy with the percolation interactive cluster growth model[24] would probably yield a more precise description for the heterogeneous percolation transition.

OBSERVATIONS OF NANOSCALE STRUCTURES AND ANOMALOUS CRYSTAL GROWTH IN SUPERCOOLED LIQUIDS

Low angle scattering from supercooled liquids in excess of that following from the compressibility has often been observed, notably by Fischer[12]. Macroscopic crystallinity usually is not seen during the experiments. The observations require one to explain how seeds can have nucleated but not have grown perceptibly. The present analysis does, in fact, suggest that some nucleation centers appear at temperatures near T_g , owing to fluctuations in driving force, but that these centers still grow rather slowly at a rate dependent on ω_{α} . While a strictly homogeneous mechanism may explain the observations, it is likely that foreign nuclei are involved in some of the experiments, since heterogeneous crystal growth is also accelerated via percolative nucleation in this regime. Fischer carefully noted in his early papers that very pure samples which were only quenched a single time to the low temperature of investigation, without being rewarmed, did not exhibit anomalous scattering. Heterogeneous initiation would explain the ability to make such so called “cluster-free” samples quite nicely.

Since the nanocrystallites grow by a dynamical percolation or chain reaction process, the embedded nanocrystallites are expected to be finite initially, but have a fractal shape. Eventually they will form a web that may be quite sparsely connected. In the early stages, particles near the nanocrystals will rotate more slowly than would be expected in the “bulk” supercooled liquid. Fractal nanocrystallites provide very long-lasting heterogeneities that will relax on times much larger than ω_{α}^{-1} which otherwise would be the natural time scale of environmental renewal in the absence of crystallization. The large exchange times seen in some single molecule experiments are easily explained in this way. Predicting the precise magnitude of $\omega_{\text{exch}}/\omega_{\alpha}$, however, requires further theoretical work and, more important, better experimental characterization of the preparation protocol since the size and shape of the nanocrystalline heterogeneities is preparation time dependent. It would also be interesting to redo the single molecule experiments with the protocol Fischer employed for achieving “cluster free” samples.

The precise temperatures at which the new growth mechanism on existing crystals begin, depends on the crystal amorphous surface energy σ_x . This surface energy, in turn, depends both on the crystal polymorph growing and on the

specific crystal face. Ediger’s observation that anomalous crystal growth occurs only for some polymorphs is consistent with the present arguments[16]. Those forms more prone to anomalously fast growth should have local structures more consonant with the liquid, and thus smaller σ_x according to the present theory. This agrees with Ediger’s observations[16].

The percolative character of the growth mechanism tied to α relaxations should lead to considerable directional randomization on each step. This results in less dependence of the growth rate on the Miller indices of the macroscopic crystal than for the normal crystalline growth mechanism, leading to spherulitic growth. At T_g percolative nanocrystallite nucleation is predicted to increase the rate of crystal surface growth by $\omega_{M\nu}^{\text{hetero}}/\omega_{\alpha} \sim 4$ orders of magnitude, in good agreement with the observed speed up in crystal growth[14].

It is interesting to note that spherulitic growth like that studied in the laboratory near T_g has also been observed in the geological context. Spheres of crystalline minerals with fibrous arrangements of crystallites are found both embedded in volcanic glasses and as free rocks which have sometimes been (in all likelihood) misinterpreted as unnatural artifacts[25–27].

IMPLICATIONS

The dynamical mosaic of RFOT theory has implications for many kinds of phase transitions in glass forming substances. Our arguments are based merely on the existence of an energy gap in the local minimum spectrum so they are thus equally appropriate for any first order transition. In mixtures phase separation into components may also occur without or along with crystallization. If the liquid is quenched deeply into the binodal for demixing, the analysis of phase separation should be quite parallel to the present one for crystallization. On the other hand, near a critical point for phase separation, the length scale of the critical composition fluctuations enters. How this length (which grows as the critical point is approached) competes with the RFOT mosaic length scale requires a more elaborate analysis. Such an analysis could be based on coupling the dynamical Landau-Ginzburg theory with the fluctuating version of the mobility transport equations proposed by one of us recently[28].

The topic of polyamorphism i.e. the existence of multiple noncrystalline phases, has engendered much spirited discussion[29, 30]. Some models of the glass transition based on frustrated phase transitions connect directly to the existence of polyamorphism[31]. The simplest Hamiltonian model of a frustrated phase transition, the so-called Brazovskii Hamiltonian for stripe formation, indeed is predicted to have both a first order polyamorphic transition, à la Brazovskii[32], and a mean field random first order transition, à la Schmalian and Wolynes[33]. The present ideas should illuminate the relations between those two transitions in stripe glass forming systems.

The present argument also raises some cautionary points

about polyamorphism. First, the ubiquity of nanocrystallite formation at deep undercooling means that the observation of a nonfaceted, overall isotropic drop of a second phase in a supercooled liquid may reflect the formation of a disoriented tangle of nanocrystalline fibers. Several of the cause célèbre substances that have been thought to exhibit polyamorphism, triphenyl phosphite and butanol for example, seem to actually be examples of such poly-nanocrystalline tangles: the Raman vibrational spectra of the spherical inclusions, are identical to the crystal[34], and the x-ray diffraction of those inclusions matches closely a linear combination of those for a nanocrystalline powder and a truly aperiodic isotropic liquid[35].

Other examples of polyamorphism such as water, are on stronger footing since they are inspired by the undoubted existence of distinctly different amorphous samples prepared by vapor deposition (high and low density amorphous ices[29]) or by pressure-induced amorphization[36]. Yet again, the relation of the new amorphous phases prepared via strongly nonequilibrium routes to any extrapolated equilibrium supercooled liquid may well be complicated by the intervention of the rapidly nucleating crystal phase at low specific configurational entropy. Indeed, if the extrapolated liquid-liquid transition occurs below the nanocrystallite formation limit discussed here there may be in principle difficulties in directly testing such extrapolations.

We see the dynamically corrected nucleation arguments put forward by Turnbull break down at low temperatures. Yet most of the practical implications of Turnbull's arguments remain intact under our revision of his crystal nucleation ideas: a substance with low melting point compared to glass transition will not only nucleate slowly in the conventional way but will also have a hard time accessing percolative nanocrystallization. Eutectics remain the best candidates for glass formation just as Turnbull suggested. In a similar way, protein folding, when the driving force is strong enough, can kinetically decouple from trap escape through a percolation mechanism like that discussed here[5, 37, 38]. Still, the fastest folders must have evolved to avoid traps, even while it is true that slow folders eventually will make it to the folded state, anyway. In general the strongly stabilized, pseudo downhill folding envisioned in this scenario is not the most common for proteins that have been studied so far in the laboratory. While strictly downhill folding is not expected to be the dominant mode of natural protein folding according to current models, this pseudo downhill mechanism may be more common.

Finally we note that an understanding of the percolative nanocrystallization kinetics may allow the synthesis of new materials via special heat treatments. The resulting nanoporcelains may have useful mechanical, electrical and magnetic properties.

Support from NIH grant 5R01GM44557 is gratefully acknowledged.

-
- [1] Rogers, A. F. A review of the amorphous minerals. *J. Geology* **25**, 515–541 (1917).
 - [2] Greet, R. J. & Turnbull, D. Glass transition in o-terphenyl. *J. Chem. Phys.* **46**, 1243–1251 (1967).
 - [3] Chaudhari, P. & Turnbull, D. Structure and properties of metallic glasses. *Science* **199**, 11–21 (1978).
 - [4] Duwez, P. Structure and properties of alloys rapidly quenched from liquid state. *Asm Transactions Quarterly* **60**, 607 (1967).
 - [5] Bryngelson, J. D., Onuchic, J. N., Socci, N. D. & Wolynes, P. G. Funnels, pathways, and the energy landscape of protein-folding - a synthesis. *Proteins - Struct. Function Genetics* **21**, 167–195 (1995).
 - [6] Lubchenko, V. & Wolynes, P. G. Theory of structural glasses and supercooled liquids. *Ann. Rev. Phys. Chem.* **58**, 235–266 (2007).
 - [7] Ediger, M. D. Spatially heterogeneous dynamics in supercooled liquids. *Ann. Rev. Phys. Chem.* **51**, 99–128 (2000).
 - [8] Russell, E. V. & Israeloff, N. E. Direct observation of molecular cooperativity near the glass transition. *Nature* **408**, 695–698 (2000).
 - [9] Mackowiak, S. A., Herman, T. K. & Kaufman, L. J. Spatial and temporal heterogeneity in supercooled glycerol: Evidence from wide field single molecule imaging. *J. Chem. Phys.* **131**, 244513 (2009).
 - [10] Berthier, L. *et al.* Direct experimental evidence of a growing length scale accompanying the glass transition. *Science* **310**, 1797–1800 (2005).
 - [11] Capaccioli, S., Ruocco, G. & Zamponi, F. Dynamically correlated regions and configurational entropy in supercooled liquids. *J. Phys. Chem. B* **112**, 10652–10658 (2008).
 - [12] Fischer, E. W. Light-scattering and dielectric studies on glass-forming liquids. *Physica A* **201**, 183–206 (1993).
 - [13] Zondervan, R., Kulzer, F., Berkhout, G. C. G. & Orrit, M. Local viscosity of supercooled glycerol near T_g probed by rotational diffusion of ensembles and single dye molecules. *Proc. National Acad. Sci. United States Am.* **104**, 12628–12633 (2007).
 - [14] Hikima, T., Hanaya, M. & Oguni, M. Microscopic observation of a peculiar crystallization in the glass transition region and beta-process as potentially controlling the growth rate in triphenylethylene. *J. Mol. Struct.* **479**, 245–250 (1999).
 - [15] Hikima, T., Adachi, Y., Hanaya, M. & Oguni, M. Determination of potentially homogeneous-nucleation-based crystallization in o-terphenyl and an interpretation of the nucleation-enhancement mechanism. *Phys. Rev. B* **52**, 3900–3908 (1995).
 - [16] Sun, Y., Xi, H. M., Chen, S., Ediger, M. D. & Yu, L. Crystallization near glass transition: Transition from diffusion-controlled to diffusionless crystal growth studied with seven polymorphs. *J. Phys. Chem. B* **112**, 5594–5601 (2008).
 - [17] Lubchenko, V. & Wolynes, P. G. Theory of aging in structural glasses. *J. Chem. Phys.* **121**, 2852–2865 (2004).
 - [18] Stevenson, J. D., Walczak, A. M., Hall, R. W. & Wolynes, P. G. Constructing explicit magnetic analogies for the dynamics of glass forming liquids. *J. Chem. Phys.* **129**, 194505 (2008).
 - [19] Stevenson, J. D., Schmalian, J. & Wolynes, P. G. The shapes of cooperatively rearranging regions in glass-forming liquids. *Nature Phys.* **2**, 268–274 (2006).
 - [20] Biroli, G., Bouchaud, J.-P., Cavagna, A., Grigera, T. S. & Verrocchio, P. Thermodynamic signature of growing amorphous order in glass-forming liquids. *Nature Phys.* **4**, 771–775 (2008).
 - [21] Tracht, U. *et al.* Length scale of dynamic heterogeneities at the

- glass transition determined by multidimensional nuclear magnetic resonance. *Phys. Rev. Lett.* **81**, 2727–2730 (1998).
- [22] Xia, X. & Wolynes, P. G. Microscopic theory of heterogeneity and nonexponential relaxations in supercooled liquids. *Phys. Rev. Lett.* **86**, 5526–5529 (2001).
- [23] Stevenson, J. D. & Wolynes, P. G. On the surface of glasses. *J. Chem. Phys.* **129**, 234514 (2008).
- [24] Anderson, S. R. & Family, F. Percolation in an interactive cluster-growth model. *Phys. Rev. A* **38**, 4198–4204 (1988).
- [25] Kirkpatrick, R. J. Crystal-growth from melt - review. *Am. Mineralogist* **60**, 798–814 (1975).
- [26] Smith, R. K., Tremallo, R. L. & Lofgren, G. E. Growth of megaspherulites in a rhyolitic vitrophyre. *Am. Mineralogist* **86**, 589–600 (2001).
- [27] Stirling, M. W. Solving mystery of mexicos great stone spheres. *National Geographic* **136**, 295–300 (1969).
- [28] Wolynes, P. G. Spatiotemporal structures in aging and rejuvenating glasses. *Proc. Natl. Acad. Sci. U.S.A.* **106**, 1353–1358 (2009).
- [29] Mishima, O. & Stanley, H. E. The relationship between liquid, supercooled and glassy water. *Nature* **396**, 329–335 (1998).
- [30] Wilding, M. C., Wilson, M. & Mcmillan, P. F. Structural studies and polymorphism in amorphous solids and liquids at high pressure. *Chem. Soc. Rev.* **35**, 964–986 (2006).
- [31] Tarjus, G., Kivelson, S. A., Nussinov, Z. & Viot, P. The frustration-based approach of supercooled liquids and the glass transition: a review and critical assessment. *J. Phys.: Cond. Matt.* **17**, R1143–R1182 (2005).
- [32] Brazovskii, S. A. Phase-transition of an isotropic system to an inhomogeneous state. *Zh. Éksp. Teor. Fiz.* **68**, 175–185 (1975).
- [33] Schmalian, J. & Wolynes, P. G. Stripe glasses: Self-generated randomness in a uniformly frustrated system. *Phys. Rev. Lett.* **85**, 836–839 (2000).
- [34] Wypych, A., Guinet, Y. & Hedoux, A. Isothermal transformation of supercooled liquid n-butanol near the glass transition: Polyamorphic transitions in molecular liquids investigated using Raman scattering. *Phys. Rev. B* **76**, 144202 (2007).
- [35] Shmyt'ko, I. M., Jim'enez-Riob'oo, R. J., Hassaine, M. & Ramos, M. A. Structural and thermodynamic studies of n-butanol. *Journal of Physics: Condensed Matter* **22**, 195102 (2010).
- [36] Mishima, O., Calvert, L. D. & Whalley, E. Melting ice-I at 77-K and 10-kbar - a new method of making amorphous solids. *Nature* **310**, 393–395 (1984).
- [37] Shen, T. Y., Zong, C. H., Portman, J. J. & Wolynes, P. G. Variationally determined free energy profiles for structural models of proteins: Characteristic temperatures for folding and trapping. *J. Phys. Chem. B* **112**, 6074–6082 (2008).
- [38] Naganathan, A. N., Doshi, U. & Munoz, V. Protein folding kinetics: Barrier effects in chemical and thermal denaturation experiments. *J. Am. Chem. Soc.* **129**, 5673–5682 (2007).